IOP PUBLISHING JOURNAL OF PHYSICS D: APPLIED PHYSICS

J. Phys. D: Appl. Phys. **41** (2008) 033001 (14pp) doi:10.1088/0022-3727/41/3/033001

TOPICAL REVIEW

In situ non-linear spectroscopic approaches to understanding adsorption at mineral–water interfaces

Simon Schrödle[1] **and Geraldine L Richmond**[1,2]

[1] Department of Chemistry, University of Oregon, Eugene, OR 97403, USA
[2] Materials Science Institute, University of Oregon, Eugene, OR 97403, USA

E-mail: richmond@uoregon.edu

Received 2 October 2007, in final form 18 October 2007
Published 14 January 2008
Online at stacks.iop.org/JPhysD/41/033001

Abstract

Over the last decades, significant advances have been made in the study of adsorption processes at mineral–water interfaces. In particular, surface-enhanced infrared (IR) techniques, and, more recently, non-linear vibrational sum-frequency spectroscopy have provided novel insights into the structure and dynamics of these interfaces. The driving forces behind adsorption at mineral substrates are as diverse as the set of commonly encountered adsorbates, which range from simple inorganic ions to organic molecules from the smallest to the largest polymers. Electrostatics, cooperative processes, self-assembly into mesoscopically ordered aggregates and specific chemical interactions all play an important role. In this topical review, particular consideration is given to organic adsorbates including surfactants, because of their eminent technological importance for the modification of surface properties and their omnipresence in the environment. This review demonstrates that non-linear optical methods greatly extend the well-established linear IR techniques and provide many opportunities for surface science to advance our understanding of the structure and dynamics of mineral–water interfaces.

(Some figures in this article are in colour only in the electronic version)

1. Introduction

Surface phenomena have attracted the interest of numerous investigators since the beginning of the 20th century. Still today, this field is an exciting area of research, with the focus progressing from simple systems, e.g. the adsorption of gases at inert surfaces, to more complex systems such as the liquid–gas or solid–liquid interfaces. Mineral–water interfaces are a particular challenge because of the often strong solid–liquid interaction and the microscopically heterogeneous nature of many minerals. Preferential dissolution and hydration of surface ions, chemical modification of the surface and pH all affect the often delicate balance of forces at the mineral–water boundary. For a long time, a more detailed investigation of such buried interfaces has been hindered by the lack of suitable experimental methods, which need to provide information at the molecular and atomic levels. High surface specificity is needed to allow the response of molecules close to the interface to be separated from an overwhelming number of similar molecules in the adjacent bulk phases. Only in the last two decades have powerful methods become more readily available with the introduction and broader application of x-ray photoelectron and auger spectroscopy [1], x-ray and neutron scattering [2], neutron reflection, scanning tunnelling and atomic force microscopy (STM/AFM), electron spin resonance (ESR), ellipsometry [3], surface-enhanced linear infrared (IR) and fluorescence techniques [4] and non-linear optical spectroscopies [5, 6]. These methods can be classified into two categories, one that requires ultrahigh vacuum (UHV) conditions or invasive sample preparation procedures, and the other, comprising methods which allow the *in situ* investigation of the solid–liquid interface.

Unfortunately, studies of the solid–liquid interface in UHV [7] have significant limitations, particularly for examining time-dependent phenomena. This makes the use of *in situ* methods highly desirable, and together with STM/AFM, optical spectroscopies are the most commonly employed techniques [6].

Fluorescence spectroscopic studies [4] are popular for characterizing adsorbate layers at solid–liquid interfaces and can identify compounds on mineral surfaces. By application of time-resolved spectrometers and statistical data analysis, aggregation numbers of surface assemblies can be determined [8]. Surface-enhanced (linear) IR methods have proven useful to determine the thermodynamic surface excess *in situ*, and offer, with the high sampling speed of state-of-the-art Fourier-transform instruments, great opportunities for kinetic studies [9]. Structurally more detailed information can be obtained by polarized IR spectroscopy [10], and, in particular, non-linear optical techniques, second-harmonic generation (SHG) and vibrational sum-frequency spectroscopy (VSFS). The latter two are inherently surface specific, and the coherent nature of the underlying non-linear optical processes can reveal more detailed information compared with linear IR techniques [11, 12]. With the aid of polarization-resolved VSFS, the molecular orientation of adsorbate molecules at interfaces can be determined [13–16].

Despite all of these efforts, our understanding of adsorption at mineral–water interfaces is still far from complete, and the importance of such adsorption phenomena in a variety of fields is reflected in the diversity of approaches, models and opinions. This topical review therefore mainly focuses on advances in optical spectroscopic techniques, with emphasis on *in situ* and non-linear methods. The structure of adsorbate layers and interfacial water molecules under equilibrium conditions will be discussed. This will be followed by a description of time-dependent measurements that are beginning to provide important new insights into adsorption dynamics.

2. VSFS background

2.1. Sum-frequency generation at interfaces

Since the general theory of sum-frequency generation at interfaces has been treated in detail elsewhere [11, 17–22], only an overview of the essential concepts for its application to mineral–water interfaces is necessary here.

VSFS is based on a three-wave mixing process, where two incident laser beams of frequencies ω_{IR} and ω_{VIS} mix to generate sum-frequency photons at $\omega_{\mathrm{SF}} = \omega_{\mathrm{IR}} + \omega_{\mathrm{VIS}}$ (figure 1).

For the experiment, pulsed laser beams are used, where ω_{IR} is tunable in the IR wavenumber range and ω_{VIS} is fixed. Spatial and temporal overlap of the beams is established at the interface and the local fields $E(\omega_{\mathrm{IR}})$ and $E(\omega_{\mathrm{VIS}})$ are then coupled by the surface non-linear susceptibility $\chi^{(2)}$ (equation (1)) to induce a non-linear polarization at ω_{SF} (figure 1).

$$P_{\mathrm{SF}}(\omega_{\mathrm{SF}}) = \chi^{(2)} : E(\omega_{\mathrm{VIS}})E(\omega_{\mathrm{IR}}). \tag{1}$$

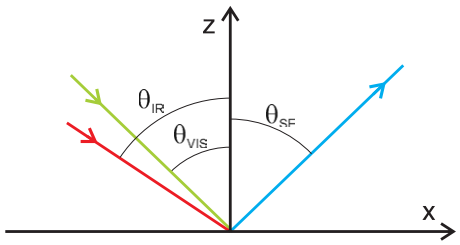

Figure 1. Sum-frequency generation by the non-linear polarization sheet of the interface located in the x–y plane. Fundamental waves (IR: red, VIS: green) are incident at angles θ_{IR} and θ_{VIS}, respectively. The SF beam is reflected at θ_{SF}. (Colour online.)

This process is coherent, and the emission of sum-frequency light is highly directional, with $\omega_{\mathrm{SF}} \sin\theta_{\mathrm{SF}} = \omega_{\mathrm{IR}} \sin\theta_{\mathrm{IR}} + \omega_{\mathrm{VIS}} \sin\theta_{\mathrm{VIS}}$, as determined by the phase matching condition at the interface between two media.

The wavelength of the visible beam is chosen to be off resonance, thus $\chi^{(2)}$ only depends on the IR frequency, and measured sum-frequency spectra for a given beam geometry are of the form

$$I_{\mathrm{SF}}(\omega_{\mathrm{IR}}) \propto |P_{\mathrm{SF}}|^2 \propto |\chi^{(2)}|^2 I_{\mathrm{VIS}} I_{\mathrm{IR}} L_{\mathrm{SF}}^2 L_{\mathrm{VIS}}^2 L_{\mathrm{IR}}^2, \tag{2}$$

I_{VIS} and I_{IR} denote the intensities of the incident beams and the L terms are the geometric Fresnel factors.

Phenomenologically, $\chi^{(2)}$ is treated as a coherent superposition of a non-resonant part $\chi^{(2)}_{\mathrm{NR}}$ and ν resonant components of the susceptibility, $\chi^{(2)}_{\mathrm{R},\nu}$ (equation (3)).

$$\chi^{(2)} = \chi^{(2)}_{\mathrm{NR}} + \sum_{\nu} \mathrm{e}^{\mathrm{i}\gamma_\nu} \chi^{(2)}_{\mathrm{R},\nu}. \tag{3}$$

Interference between the individual resonant contributions is accounted for by a relative phase γ_ν.

It can be readily shown that $\chi^{(2)}$ of bulk phases vanishes in centrosymmetric media, if contributions from magnetic dipoles are neglected [5, 17]. Therefore, only molecules with a net orientation towards the interface can contribute to $\chi^{(2)}$, and this is the origin of the inherent surface specificity of VSFS.

Typically, $\chi^{(2)}_{\mathrm{NR}}$ is real for common dielectric surfaces and can be considered constant over a limited frequency band [23], but $\chi^{(2)}_{\mathrm{R},\nu}$ is a complex quantity, and its tensorial components in the surface-fixed axis system i, j and k can be macroscopically described as a Lorentzian [13, 24]

$$(\chi^{(2)}_{\mathrm{R},\nu})_{ijk} \propto \frac{A_k M_{ij}}{\omega_{\mathrm{IR}} - \omega_\nu + \mathrm{i}\Gamma_\nu}. \tag{4}$$

In equation (4), A_k is the IR transition moment and M_{ij} the Raman transition probability of mode ν, characterized by a resonant frequency ω_ν and the natural line width Γ_ν. Accordingly, a sum-frequency response can only be observed for modes which are both IR and Raman active.

To relate molecular-scale structure to the macroscopic observables, a way has to be devised to derive $\chi^{(2)}_{ijk}$ from the (microscopic) hyperpolarizabilities of interfacial molecules. Unfortunately, even for linear optical properties of condensed phases, such calculations still remain a challenge after almost a century of research. Therefore, only a first-order

approach is feasible at present for the discussion of sum-frequency data, and commonly the interfacial region is treated as an ensemble of non-interacting molecular second-order hyperpolarizabilities $\beta^{(2)}_{lmn}$. With l, m and n representing the inertial frame of the molecules, we can write

$$\chi^{(2)}_{ijk} = \sum_{\text{molecule}} \beta^{(2)}_{ijk} = N\langle\beta^{(2)}_{ijk}\rangle,$$

$$\text{with} \quad \beta^{(2)}_{ijk} = \sum_{lmn} u_{ijk:lmn}\beta^{(2)}_{lmn}. \tag{5}$$

In equation (5), the coefficients for the Cartesian components, $u_{ijk:lmn}$, relate the $\beta^{(2)}$ tensor elements in the molecular frame to those in the interface-fixed system [25]. Using the orientational average $\langle\,\rangle$, the orientation of interfacial molecules with respect to the interface can be extracted from the transformation tensor $u_{ijk:lmn}$.

At the mineral–water boundary, the interfacial layer can often be approximated by an isotropic plane, corresponding to $C_{\infty v}$ symmetry. From the invariance of $\chi^{(2)}_{ijk}$ under the symmetry operations of $C_{\infty v}$ it can then be shown that only 7 of the 27 tensor elements of $\chi^{(2)}$ are non-zero and of these, only 4 are unique. With the lab coordinates chosen so that z lies along the interface normal and that the xz-plane is the plane of incidence (figure 1), they are $\chi^{(2)}_{xxz} = \chi^{(2)}_{yyz}$, $\chi^{(2)}_{xzx} = \chi^{(2)}_{yzy}$, $\chi^{(2)}_{zxx} = \chi^{(2)}_{zyy}$ and $\chi^{(2)}_{zzz}$. In addition, for ω_{VIS} far from resonance, $\chi^{(2)}_{xzx} = \chi^{(2)}_{yzy} = \chi^{(2)}_{zxx} = \chi^{(2)}_{zyy}$. These elements can be probed using combinations of incident and reflected linearly polarized light [11], namely: *ssp*, *sps* (or *pss*) and *ppp*, where the letters represent light polarized parallel to the plane of incidence (p) or perpendicular to the plane of incidence (s). According to a widely accepted convention, all polarization notations are given in the order: sum-frequency, visible, IR.

2.2. Spectral decomposition

Compared with linear IR spectra, the deconvolution of VSFS spectra $I_{\text{SF}}(\omega_{\text{IR}})$ is typically more difficult because of the complex nature of the data and the interference of overlapping resonances. The most basic approach is to assume a Lorentzian distribution of energies (equation (4)) for the individual bands, but it is not always possible to obtain satisfying fits using this approximation [11]. Such discrepancies were often attributed to inhomogeneous broadening, and a Gaussian distribution of vibrational frequencies ω_ν, with centre frequency ω_{ν_0}, is commonly chosen [26–28]

$$\chi^{(2)}_{\text{R},\nu} = B_\nu \int \frac{1}{\omega_{\text{IR}} - \omega_\nu + \text{i}\Gamma_\nu} \exp\left[-\frac{(\omega_\nu - \omega_{\nu_0})^2}{\Delta^2_\nu}\right] \text{d}\omega_\nu. \tag{6}$$

In equation (6), B_ν is the effective sum-frequency transition strength of the ν^{th} band, Δ_ν accounts for inhomogeneous broadening. Note that for most resonances at the mineral–water interface $\Delta_\nu \gg \Gamma_\nu$, therefore the peak shape is often not sensitive to Γ_ν, which has therefore frequently been treated as a constant during spectral fitting [29].

3. Non-linear spectroscopy at buried interfaces

The range of experimental tools available for the study of a buried interface depends to a large extent on the nature of the adjacent bulk phases [30]. A variety of methods exist for the investigation of solid–UHV interfaces [7, 31, 32] and have been applied to numerous substrates, including metal oxides and ionic compounds [7,33]. Spectroscopic approaches rely on the interaction of the interface with electrons or photons of various energy content. Electrons need a virtually free path to the interface, whereas photons, depending on their wavelength, may interact with condensed bulk phases in ways such as adsorption, scattering or ionization. These complications often make the investigation of buried interfaces a challenging endeavor. Furthermore, spectroscopic signatures of the bulk phase have to be separated from effects caused by the relatively small number of interfacial molecules for some methods. Despite these limitations, linear optical techniques, e.g. vibrational spectroscopy, often are superior to other experimental approaches by being non-destructive and comparatively fast. With a variety of commercial bench-top instruments available, they have delivered valuable information about interfaces [34–45]. But the stronghold of linear IR spectroscopy is the determination of adsorbate species and adsorption isotherms rather than more detailed elucidation of the interfacial water structure, which is important for the understanding of equilibrium phenomena such as overcharging [46] or dynamic properties of water–mineral interfaces. Using non-linear optical methods, interference from most bulk phases can be minimized, opening up a new field of research which has ever been expanding over the last two decades.

As far as VSFS is concerned, directing the visible beam to the interface is often straightforward because at least one of the phases adjacent to the interface is commonly transparent at visible frequencies. For the IR beam there are two options, either with the beam entering from the liquid or from the solid phase. Because of the strong absorption of water at IR frequencies, the first method necessitates a very thin liquid layer, but can be the only way to perform studies on opaque solids. In some cases, substitution of D_2O for H_2O can be useful to access certain spectral regions [47]. For the study of adsorption processes, thin liquid layers above the solid phase can be a severe restriction, because they considerably limit mass transport. Furthermore, depletion of such a thin layer can significantly alter the bulk concentration of an adsorbate in the liquid phase, which limits experimental work to fully equilibrated interfaces.

Most of the non-linear optical studies performed so far at mineral–water interfaces took advantage of the high transparency of single-crystalline mineral phases for both IR and visible light, and except for few cases [48], a co-propagating geometry of VIS and IR beams was chosen [49–51] Ultrathin solid films [52] deposited on suitable substrates can also be studied by this approach. Beam propagation within the phase of higher optical density also has the inherent advantage that a beam geometry just above the critical angle for total internal reflection (TIR) can be used.

As can be derived from the Fresnel equations, this considerably increases the signal level [11].

4. The neat mineral–water interface

Adsorption of surfactants at a neat mineral–water interface results in the replacement of some or all of the surface-coordinated water molecules in addition to altering the hydrogen-bonding structure of the interfacial region. Therefore, a comprehensive understanding of the neat mineral–water boundary is a prerequisite for any discussion of adsorption phenomena.

With recent experimental and theoretical studies of these interfaces, an insightful picture has begun to emerge [2]. Whereas the structural properties of the solid phase remain almost unaltered up to the very topmost layer, water, as a liquid phase, undergoes more significant structural changes at longer distances from the interface. These changes are, in part, induced by what is commonly referred to as 'hard-wall' effect: the formation of particularly ordered layers near a surface due to the geometrical constraints of the solid–liquid boundary acting upon water molecules. Additionally, electrostatic effects play a key role at mineral–water interfaces. Oxide minerals are known to exhibit electrical fields of considerable strength at their surfaces [53]. Ionic solids often show preferential dissolution of ions, rendering the surface highly charged [54].

X-ray scattering [2] and quasi-elastic neutron scattering (QENS) [55–60] have recently been employed for the study of water layers on mineral substrates. The majority of these studies, however, were performed on the mineral–water vapour interface rather than the mineral–water interface because of the experimental constraints imposed by QENS. Such studies are certainly highly relevant for moist geochemical environments and of great theoretical value, but substantial differences in interfacial structures of a solid in contact with water vapour compared with a bulk liquid phase can be anticipated, in particular for the typically only two molecular water layers present in QENS samples [57–59].

For the vast majority of minerals relevant to the study of adsorption processes, e.g. metal oxides [52, 61, 62] or ionic crystals [54], the presence of a macroscopic liquid phase is essential because their surface charge [61] is modulated by the pH of the bulk solution. Since many of these minerals are semi-soluble in aqueous environments, the equilibrium hydration structures of dissolved and surface bound ions cannot be expected to be the same for only a thin layer of water as opposed to liquid water.

VSFS has long been used to investigate a variety of aqueous interfaces [63–66] and has revealed considerable detail about water structure adjacent to mineral substrates [48,52,54,61]. Some of these findings have been summarized in previous reports [11, 67], and in addition, we also want to briefly discuss several important aspects is this review.

A general feature of nearly all aqueous interfaces [11,48,52,54,61,68] is the existence of two major OH bands, which are typically located at ∼3200 and ∼3450 cm^{-1}. They originate from different degrees of hydrogen bonding between surface water molecules, with the lowest frequencies representative of stronger bonding. Due to the similarity of the frequencies to those of the OH resonances in the corresponding bulk phases, these bands have often been referred to as 'ice-like' or 'liquid-like' [11]. However, these terms are misleading because the vibrational frequencies reflect the hydrogen-bonding environment rather than any long-range order, which is characteristic for ice. Attempts to ascribe the low-energy (3200 cm^{-1}) band to the primary hydration layer of mineral surfaces [2] appear to be very speculative, because this band has also been reported for many interfaces which lack any lateral ordering of the solid phase. On such interfaces, an epitaxial relationship between the substrate lattice and the adjacent first water layer is unlikely and thus cannot be the molecular origin of the 3200 cm^{-1} band. In some cases, lattice matching between substrate and first hydration layer may affect the structure of interfacial water molecules and was held responsible for the (relatively small) changes of OH band positions observed by some investigators for interfaces between water and amorphous or crystalline solids, respectively [48]. It has also been shown by detailed analysis of the surface potential dependence of the OH resonances that water molecules contributing to both VSFS responses are located within an interfacial region well beyond the first and second hydration layers [66].

Based on these findings, the characteristic ∼3200 and ∼3450 cm^{-1} bands can be assigned to highly ordered water molecules with symmetric, tetrahedral coordination and more disordered asymmetrically bonded molecules [11, 54], which coexist in a broader interfacial region. Naturally, the population of these species can vary with distance from the solid substrate [29]. In this review, current evidence suggests that geometrical constraints, i.e. the reduction of the available degrees of freedom imposed by the interface upon hydrogen-bond rearrangement rather than direct substrate–water interactions, or molecules within a highly laterally ordered first hydration layer are the molecular origin for the two predominant hydrogen-bonding environments observed by VSFS.

5. Adsorption and overcharging

A number of mechanisms are known to drive adsorption processes, or generally speaking, to cause concentration enhancement of a particular species near an interface compared with the bulk phase.

It has already been noted that the majority of mineral–water interfaces carries considerable surface charge, which generates a strong electrical field across the interface. Strong fields are also present at various modified mineral surfaces, which can often be found when surface-active or reactive species form molecular layers on minerals exposed to aqueous environments containing organic matter [69, 70].

Given the prevalence of electrical fields at interfaces, electrostatics are important for most models that describe adsorption as far as ionic adsorbates are concerned. But even for relatively simple adsorbates, e.g. metal ions, classical electrostatic theories based on point charge distribution and

continuous dielectric medium theory often fail [46, 71, 72]. In particular, adsorption often continues beyond the point of charge neutrality of the interface, a phenomenon commonly referred to as overcharging [46, 71, 72]. This behaviour has important implications for colloid stability, as has been discussed by others in detail [46].

Although it appears counterintuitive at first, with advances in the theory of coulombic interactions at interfaces, in some cases overcharging can be explained by pure electrostatics [71, 73]. These theoretical approaches use a more refined description of the physics of strongly interacting charged systems, going beyond the framework of common mean-field theories, e.g. the Debye–Hückel [74] or (non-linear) Poisson–Boltzmann [71, 75] theories. Interactions among adsorbate ions or between adsorbate ions and interfacial charges are the molecular basis of these more advanced approaches. Generally, for such correlated effects to become operative, high ion valencies and high electrolyte concentration are prerequisite [46].

Since many adsorption processes occur at relatively low adsorbate (and electrolyte) concentrations, other driving forces have to be considered. Such adsorption phenomena that are not governed by electrostatics have often been termed *specific adsorption*, which includes interactions like complex formation at the interface, hydrogen bonding or even the formation of covalent bonds [46]. For the understanding of adsorption phenomena of molecules containing hydrophobic moieties, water structure mediated interactions [76] are essential.

Apart from the adsorption of inorganic (metal) ions at interfaces [62], a topic beyond the scope of this paper and only rarely [77–79] investigated by non-linear optical methods, surfactants and carboxylates are arguably the most widely studied classes of adsorbates [41, 80–82]. VSFS studies were performed on some of their typical representatives like sodium dodecyl sulfate (SDS) [49] and *n*-alkyl carboxylates [29, 49, 51, 83]. Using this surface-specific technique, adsorbate as well as interfacial water structure and orientation were determined at various degrees of surface coverage to yield a detailed picture of the different stages of adsorption at mineral–water interfaces.

6. Adsorption of small organic ions

Carboxylates of low molecular weight are ubiquitous in soils [84, 85] and their adsorption on mineral particles plays an important role in the environment [86, 87]. There are also numerous industrial processes which involve the interaction of carboxylates with mineral surfaces. The carboxylates of different alkyl chain lengths were studied for their practical relevance, but also to investigate the effect of gradually increasing the hydrophobicity of the adsorbate on interfacial structure [83]. So far, fluorite (CaF_2) has been the most commonly chosen substrate for such adsorption studies [29, 49, 51, 83]. Together with other calcium containing minerals, e.g. calcite ($CaCO_3$), scheelite ($CaWO_4$), wollastonite ($CaSiO_3$) and apatite ($Ca_5(PO_4)_3$(OH, F, Cl)), it is a highly important industrial raw material and a major fluorine resource [9]. Recovery of fluorite from mining feeds is usually performed via flotation, a widely adopted method for the concentration of minerals. Flotation relies on surface modification of mineral particles. Carboxylic acids are the most commonly used surface-active agents. Fluorite also serves as a model compound for other semi-soluble minerals, which might not be transparent in the IR, available as single crystals or otherwise easily studied by spectroscopic means. The surface chemistry of calcium minerals has been extensively investigated [88–92]. From potentiometric experiments, Wu *et al* [88, 89] were able to derive a detailed surface species distribution. Varying the pH of the bulk liquid phase changes the relative abundance of positively or negatively charged sites and therefore alters the surface charge. Additionally, preferential solvation of F^- surface ions can affect the charge balance at the CaF_2–water interface [93]. At pH values below the isoelectric point (IEP), the concentration of sites with a net positive charge increases, because of fluoride protonation at the interface [89]. At higher pH, fluoride ions are exchanged by hydroxyl ions and the population of net negatively charged sites increases. Note that the IEP can vary considerably amongst samples, and, in particular, surface carbonation can lower the IEP [93]. Reported values range from pH 6.6 to ~10. Most studies found a positively charged surface below pH 9–10 [94]. These positive charges will lead to a concentration build-up of negatively charged ions close to the interface, and therefore even the ions of the lower members of the homologous *n*-alkyl carboxylates, formate, acetate and propionate, which are not regarded surface-active, will be attracted to the interfacial region. The sum-frequency bands of both the carboxylate and alkyl functionalities were studied using VSFS [83].

The bands associated with the carboxylate head group (~1350 cm^{-1} for formate, ~1450 cm^{-1} for other carboxylates), often described only as a symmetrical νCO group mode, contain notable contributions from CH_2 and CH_3 vibrations [83]. For formate and propionate, both bands are separated well enough to allow for at least a semi-quantitative analysis, and in all cases, a steady increase in the sum-frequency response was observed with increasing bulk concentration, up to the highest concentration studied, ~333 mM. By selective deuteration of propionate adsorbed on fluorite [83], strong coupling of the carboxylate resonances with CH deformation modes could be demonstrated (figure 2). In figure 2(*a*), two distinctive bands are visible for hydrogenated propionate. For the deuterated compounds (figures 2(*b*) and (*d*)), the position of the ~1450 cm^{-1} resonance is shifted due to the changing of the CH contributions to the carboxylate resonance. These experiments also showed that the ~1477 cm^{-1} band, which is absent for propionates that lack the CH_3 group (figures 2(*b*) and (*d*)), can be attributed to a δCH_3 mode.

Unfortunately, for acetate, CH bending modes and carboxylate vibrations overlap, obscuring details of the headgroup resonances. The orientations of the methyl and carboxylate groups of acetate, however, are constrained by the geometry of the molecule. Thus, the combined amplitude of carboxylate and CH_3 deformation bands was used to quantify acetate adsorption at the fluorite–water interface [29].

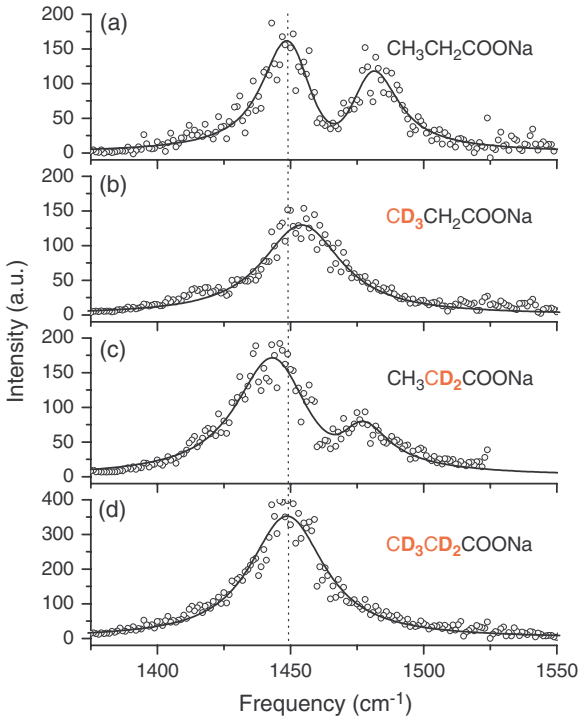

Figure 2. Comparison of VSFS spectra (ssp) of sodium propionate (aq, 333 mM) at the CaF_2 solid/liquid interface. (*a*) CH_3CH_2COONa; (*b*) CD_3CH_2COONa; (*c*) CH_3CD_2COONa; (*d*) CD_3CD_2COONa. Reprinted with permission from [83]. Copyright 2007 American Chemical Society.

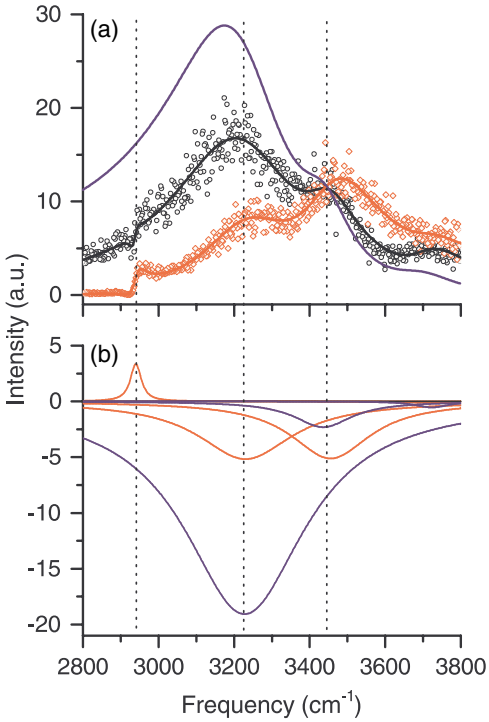

Figure 3. (*a*) VSFS spectra (ssp) of the sodium acetate (aq)/CaF_2 interface as a function of acetate concentration (from bottom to top): 333 mM (red/light grey), 77 mM (black), 0 mM (blue/dark grey, data omitted for clarity). Lines are curve fits. (*b*) Decompositions of the fit spectra at selected concentrations: 0 mM (blue/dark grey lines), 333 mM (red/light grey lines). Sign indicates relative phase of a contribution (0 or π). Reprinted with permission from [83]. Copyright 2007 American Chemical Society. (Colour online.)

The other spectral region of interest for these studies (2700–3800 cm^{-1}) covers the signatures of interfacial water molecules and of CH_2/CH_3 stretch resonances. The origin of the VSFS response of water dipoles at the neat mineral–water interface has already been discussed. The amplitudes of the main water modes located at ∼3200 and ∼3450 cm^{-1} were found to undergo a notable decrease with increasing acetate concentration (figures 3(*a*) and (*b*)) [83]. Furthermore, the relative abundance of tetrahedrally coordinated water molecules is shifted in favor of more asymmetrically bonded species, as indicated by the amplitudes of the individual contributions shown in figure 3(*b*). These observations were attributed to the presence of acetate ions at the interface, shielding the surface charge. Consequently, fewer water molecules experience an aligning electrical field, and unfavourable interactions between water molecules and methyl groups of acetate ions reduce the number of tetrahedrally coordinated water molecules with a net orientation towards the interface. Even at high acetate concentrations (333 mM), the interface remains positively charged, and the residual water response still amounts to over 60% of its original amplitude [83]. From this and other evidence it was concluded that orientation of water molecules extends well beyond the first molecular layer [29, 83, 95]. Apparently, the adsorbate layer of short-chain carboxylates is not dense enough to cause complete screening of the surface charge, nor do the carboxylate-substrate interactions alone lead to charge neutralization or even overcharging of the interface. The relative weakness of carboxylate-fluorite bonding in the absence of other effects which stabilize the adsorbate layer is also evident from the full reversibility of the adsorption process and the rapid dynamic equilibrium between bulk and adsorbed acetate molecules [29].

The mainly coulombic nature of the interaction of short-chain carboxylates with the fluorite substrate has also been demonstrated by a study of the pH dependence of acetate adsorption [29]. As the surface speciation undergoes pH-controlled changes, the amount of acetate detected at the interface varies considerably: the surface charge is increasingly positive below the IEP when the pH is lowered, because more positively charged protonated OH_2^+ surface species are generated [89]. Only at pH values below the pK_a of acetic acid does protonation of acetate ions lead to a rapid decrease of acetate adsorption. At pH>IEP, acetate adsorption is rendered electrostatically unfavourable by the prevalence of negatively charged surface species [29]. From the analysis of pH-dependent energy shifts of carboxylate resonances [29], it has been shown that adsorbate–adsorbate interactions are weak for fluorite-adsorbed acetate ions. The corresponding shifts of the water bands, albeit small, are noticeable and indicate that hydrogen-bonding strength of interfacial water molecules is modulated by the bulk pH.

A schematic view of the acetate(aq)/fluoride interface at an intermediate *p*H is given in figure 4. Although no strict separation should be implied, it has been concluded from a series of experiments [29] that tetrahedrally coordinated (dark blue, region (*b*)) molecules reside further away from the

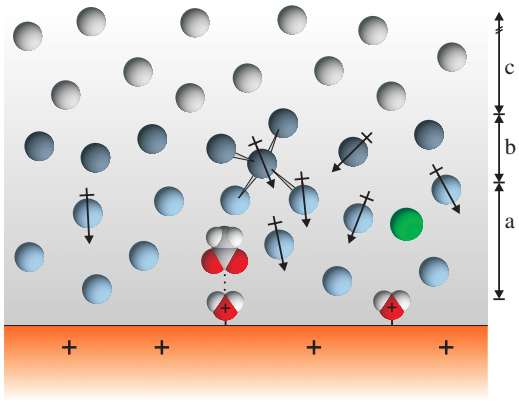

Figure 4. Schematic view of the sodium acetate(aq)-fluorite interface. Water species are represented by blue (regions a,b; see text) and gray spheres (region c; molecules with no net orientation). Acetate and chloride (green) ions are also shown. Arrows indicate the unit vector of the H_2O dipole moment. Reprinted with permission from [29]. Copyright 2007 American Chemical Society. (Colour online.)

interface, while more disordered molecules are predominantly located closer to the surface (light blue, region (*a*)). The amplitude of the latter increases markedly with decreasing *p*H due to a higher degree of orientational alignment caused by a stronger electrical field at the interface. The presence of adsorbed ions and of acetate (together with chloride ions used as a background electrolyte) in the diffuse ion layer counteracts symmetric tetrahedral water coordination, because many of these water molecules are located within or near the hydration sphere of charge-compensating anions (either chloride or unbound acetate ions). The water molecules interspersed in the ion layers close to the interface thus act as probes for the electrical field at the interface. As the ion layer balancing the surface charge becomes more diffuse further from the interface, the number of tetrahedrally coordinated water molecules oriented by the interfacial field increases (dark blue, figure 4). Over a broad range of pH values, the orienting field in this region (region (*b*), figure 4) appears to be remarkably constant due to the charge-compensating action of the electrical double layer and the adsorbed acetate, and only increases when acetate adsorption becomes unfavourable at low *p*H [29].

7. Cooperative adsorption and surface aggregation

It has long been realized that aggregation of amphiphiles is a highly cooperative process, driven by chain-chain interactions and hydrogen-bond mediated effects. In bulk liquids, a variety of associates can be formed, ranging from small micelles up to large, mesoscopically ordered systems. At interfaces, and in particular at the mineral–water boundary, geometrical constraints and substrate–headgroup interactions additionally affect the aggregation process. The type of surface aggregates formed critically depends on the interplay of these interactions. Accordingly, aggregation of adsorbates can lead to a number of different structures, and monolayers, bilayers, as well as adsorbed micellar entities (admicelles) have been observed [41, 96]. At intermediate levels of adsorption, the interfacial plane has often been reported to be microheterogeneous, with regions of densely adsorbed layers interspersed with areas of much lower coverage.

The importance of hydrophobic effects for the formation of surface aggregates has frequently been discussed, but at low surface concentrations, adsorption is mainly driven by electrostatics [51]. Using VSFS, the electric field at the interface can be probed by analyzing the response of interfacial water molecules, which align, in thermal equilibrium, with their dipolar axes along the field. Upon addition of surfactant to the liquid phase at concentrations far below the threshold for cooperative adsorption, a strong decrease of the second-order susceptibility arising from these water molecules indicates that a considerable number of surfactant molecules are adsorbed at the interface well before the formation of well-ordered aggregates commences. These states of adsorption are characterized by a high degree of disorder. This leads to a near-zero orientational average of their molecular hyperpolarizabilities and consequently only very weak signals from these adsorbate-specific bands which are otherwise very strong at higher surface coverage. But the presence of electrostatically adsorbed molecules is of great importance for adsorption kinetics, as the adsorbed monomers act as nucleation sites for further adsorption when the bulk concentration is increased. Evidence for these mechanistic aspects has so far only been derived from other experimental methods [97, 98]. Non-linear optical methods have the potential to make significant further contributions in this area.

The sensitivity of the interfacial water structure towards surfactant adsorption at the mineral–water interface has been demonstrated by VSFS for a number of adsorbates. At the interface, the energetic effect of water on adsorption equilibria is very significant, but has often been neglected because of the difficulties associated with the identification and measurement of interfacial water molecules. At mineral surfaces, strong electric fields in addition to specific interactions of surface ions with water molecules can lead to a strong local ordering (orientational alignment with respect to interface) of water molecules [99], which affects kinetics as well as thermodynamics of surfactant adsorption.

7.1. Carboxylate monolayers

Apart from the overall morphology of the surface aggregates and their effect upon the electrostatic balance and hydrogen-bonding structure near the interfacial region, the conformational order within such assemblies plays a key role in their stability and interactions with the adjacent liquid phase. From non-linear optical spectroscopy, considerable detail on the conformational order of surface-bonded aggregates has been revealed by a number of studies [51, 100, 101]. For such investigations, the methylene sum-frequency response of the surfactant's alkyl chain is of particular value, because the prevalence of gauche defects can be determined by exploiting the properties of the second-order optical process [49]. In addition to the carboxylates already discussed above, more hydrophobic adsorbates, namely hexanoate (C_6), dodecanoate (C_{10}) and stearate (C_{18}) have also been studied at the fluorite–water interface [51] and are characterized by

a high conformational degree of freedom of the alkyl chain compared with their short-chain homologues (e.g. acetate). Their surface affinity and thus their ability to neutralize surface charge was found to be highly dependent on the chain length of the carboxylate ions. The range of concentrations where charge neutralization was achieved spans a concentration range of 5 orders of magnitude, from above 333 mM for acetate (interface still positively charged), to 18 μM for stearate. Adsorption of carboxylates containing 10 or more carbon atoms was found to proceed well beyond charge neutrality, thus causing charge reversal and a flip of the prevalent orientation of water molecules at the interface [51]. For the longer-chain carboxylates, a strong response from terminal CH_3 groups has been reported, accompanied by a lack of any CH_2 signals. Becraft *et al* [51] attributed these observations to the formation of tightly packed, well-ordered monolayers with all-trans conformation of the alkyl backbone. Water molecules hardly penetrate into such hydrophobic layers, and VSFS revealed the presence of weakly bound, uncoupled OH oscillators adjacent to self-assembled stearate or oleate monolayers at saturation coverage [51]. Such water molecules are typical for abrupt, strongly hydrophobic interfaces.

Compared with micellization kinetics in bulk liquid phases, the formation of molecular layers with a well-defined orientation towards the interface and a high degree of conformational alignment is a relatively slow process, with a characteristic time on the order of hours [51]. Non-linear optical spectroscopy has so far only rarely been used for the investigation of kinetic phenomena at mineral–water interfaces in general. Becraft *et al* [51] reported spectra of stearate at the CaF_2–water interface as a function of time and presented spectra recorded 2, 3, 4 and 24 h after an increase in bulk concentration above the critical concentration which initiates the self-assembly process at the interface (figure 5). Over the course of hours, the initially strong water response (figure 5(*a*)) disappeared, while the sum-frequency response arising from terminal CH_3 groups of the surfactant molecules (at ~2870 and ~2930 cm^{-1}) dramatically increased (figures 5(*b*)–(*d*)). Only after 24 h is monolayer formation completed, and some degree of structuring found to return to the interfacial water molecules (band at ~3200 cm^{-1}, figure 5(*e*)). This is accompanied by a flip in orientation of the water dipoles relative to the interface, as expected from the now negatively charged adsorbate layer [51]. The steady increase of the CH_3 response over time was attributed to continued monolayer formation rather then bilayer formation, because the latter would be accompanied by a decrease of the methyl signal due to the cancellation of molecular CH_3 hyperpolarizabilities in bilayers [50].

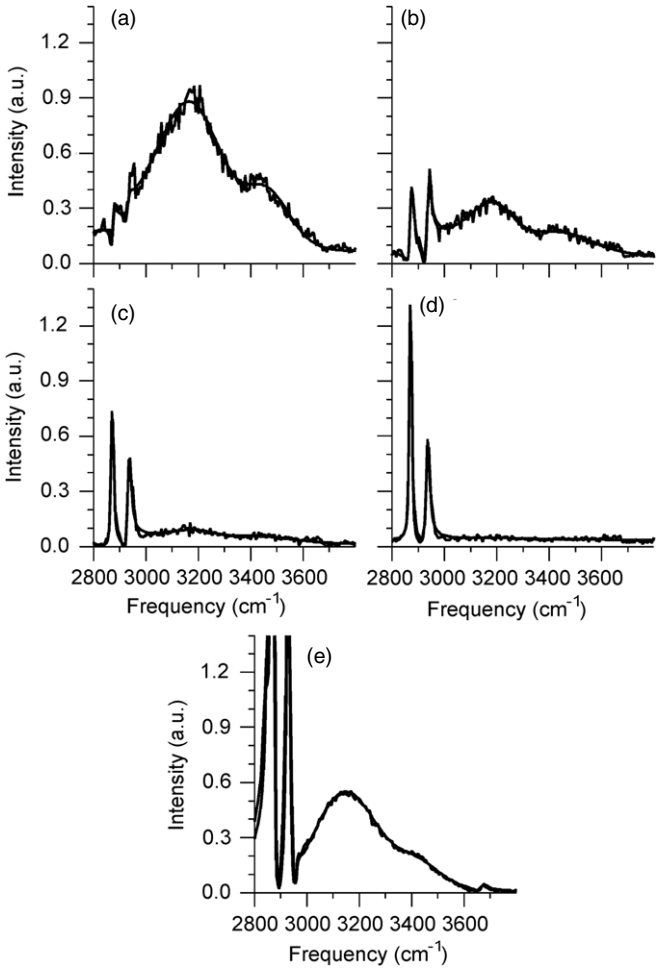

Figure 5. VSFS spectra recorded as a function of time for the CaF_2/H_2O/stearate interface following a stearate concentration increase from 12 to 19 μM. Part (*a*) was recorded immediately after the concentration increase followed by (*b*) 2 h, (*c*) 3 h, (*d*) 4 h and (*e*) 24 h. Lines are actual data, curve fits are also shown. Reprinted with permission from [51]. Copyright 2005 American Chemical Society.

7.2. *Bilayer formation*

Sodium dodecyl sulfate (SDS) is among the few surfactants other than carboxylates which have been studied at the mineral–water interface by non-linear optical methods [49,50]. Sum-frequency spectra of the sulfate headgroup were so far only reported at the air–water interface [102–104] and used to determine the molecular orientation of the SDS molecule at this interface [103, 104]. Other work mainly focused on CH modes and covers SDS adsorption at the liquid–water [95], air–water [24] and hydrophobic solid–water [105, 106] interfaces. Becraft *et al* [49, 50] used fluorite as the substrate for their study of SDS adsorption. Owing to its different molecular shape, and in particular its larger (sulfate) head group, SDS was found to exhibit distinctively different adsorption characteristics compared with alkyl carboxylates (figure 6) [51].

At low concentrations (figure 6(*a*)), the effects of SDS on the interfacial structure are very similar to carboxylate surfactants: a strong decrease of the overall response associated with interfacial water molecules spanning across the entire OH stretching region was reported [50]. Full neutralization of the initially positively charged CaF_2 substrate was observed at approximately 1/40th of the bulk CMC. At this concentration no spectral signatures of interfacial water species, including any 'free OH' oscillator bands, were detected (figure 6(*b*)). Note that at the point of charge neutralization, the CH bands are still very weak, indicating a highly disordered state of SDS molecules in the interfacial region (molecules randomly oriented towards the interface). With the SDS

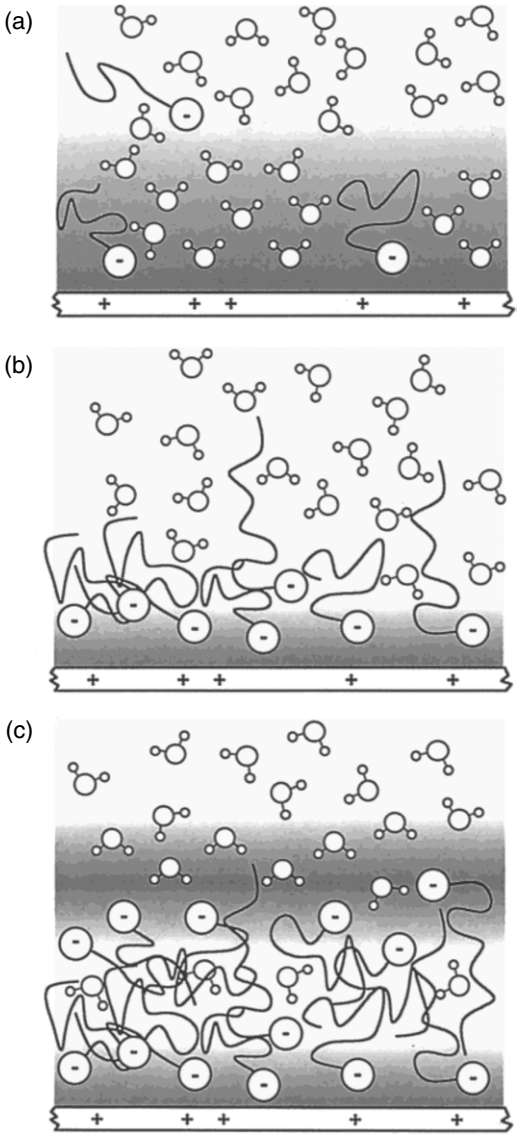

Figure 6. Diagram of the three distinct adsorption regions of SDS on CaF_2. (*a*) Monomer adsorption of anionic SDS to the positively charged CaF_2 surface, (*b*) the IEP of the CaF_2/H_2O/SDS interface and randomization of interfacial water molecule structure and (*c*) bilayer formation and charge reversal at the CaF_2/H_2O/SDS interface and the return of interfacial water structure above this layer. Reprinted with permission from [49]. Copyright 2003 American Chemical Society.

concentration further increasing, the spectral response across the OH stretching region rises again (figure 6(*c*)) [50]. Becraft *et al* [50] also performed a quantitative analysis of the CH modes as a function of SDS bulk concentration, substituting D_2O for H_2O to remove the interference of OH modes with the CH amplitudes (figure 7). Spectra of D_2O and H_2O solutions over a a range of surfactant concentrations were fit simultaneously to corroborate band energies and assignments [28]. Already at low SDS concentrations, two CH oscillators were found, at 2873 cm^{-1} and 2934 cm^{-1}, respectively. In agreement with other studies [27, 69, 105, 107, 108], these bands were assigned to the symmetric stretch of the terminal CH_3, split by Fermi resonance with an overtone of the CH_3 bending mode. Interestingly, the CH band amplitudes were

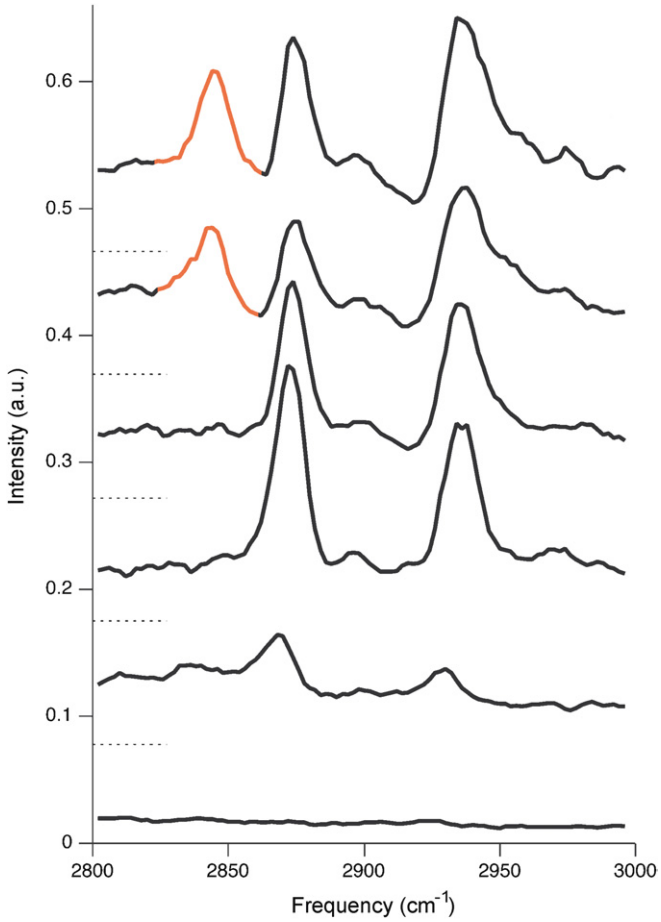

Figure 7. VSFS spectra of CaF_2/D_2O/SDS interface in the CH stretching region at the SDS concentration of (*a*) neat CaF_2/D_2O, (*b*) 1.0×10^{-4} M, (*c*) 5.0×10^{-4} M, (*d*) 1.0×10^{-3} M, (*e*) 5.0×10^{-3} M and (*f*) 9×10^{-3} M. Spectra are offset for clarity, with the zero signal level for (*b*)–(*f*) shown as a dotted line. Reproduced from [50] by permission of the PCCP Owner Societies.

found to be much smaller compared with those of the alkyl carboxylate monolayers [51] discussed before. Therefore, adsorbed SDS molecules were characterized by a lower degree of conformational order of their alkyl chains (figure 6(*c*)). At higher concentrations, the degree of orientational order of the terminal CH_3 groups increases, and also their symmetry axis was reported to be perpendicular to the interfacial plane to a larger extent [50].

Another striking difference between SDS and the related carboxylate monolayers is the decrease of the CH_3 amplitude with *increasing* bulk concentrations after a certain coverage threshold (black bands, figures 7(*a*)–(*f*)). Becraft *et al* [50] demonstrated that this amplitude decrease is due to bilayer formation and is caused by the cancellation of the molecular hyperpolarizabilities of oppositely oriented terminal CH_3 groups in the bilayer. Furthermore, elevated bulk concentrations force the adsorbate layer into a high degree of disorder, which is clearly apparent from a new peak appearing at 2849 cm^{-1} and attributed to a symmetric stretch vibration of CH_2 groups of the surfactant backbone (red band, figures 7(*e*) and (*f*)) [50]. The latter mode cancels out in the all-trans conformation of the SDS molecule prevalent at lower concentrations.

It was also shown from phase information extracted from spectral fits and by analyzing interference phenomena of VSFS modes, that SDS bilayer formation, accompanied with overcharging of the interface and an orientation of surfactant headgroups towards the bulk liquid phase, results in a flip of the predominant orientation of water molecules [49, 51].

8. Effect of electrolytes

In many systems of practical relevance, adsorption processes take place in the presence of electrolytes. In aqueous solutions, these arise from dissociated ions, which originate from the dissolution of the semi-soluble minerals itself as well as from other sources. In fact, most aqueous systems in environment, industry and biology contain a considerable amount of dissolved ionic solids. Even without considering any specific interactions between inorganic ions and mineral surfaces [109, 110], electrostatic attraction or repulsion of ions by interfacial fields will lead to screening of surface charges. This will greatly affect the structure of the interfacial region compared with the neat mineral–water boundary [111]. So far, only a very limited number of studies used non-linear optical methods to investigate the effect of electrolytes on interfacial phenomena at mineral surfaces. The current knowledge has largely been derived from electrokinetic data as well as methods based on x-ray spectroscopic and scattering [2] techniques, which are particularly useful to study the adsorption of heavy metal ions [112, 113].

In addition to changes in the layer adjacent to the solid substrate, electrolytes can alter the surface speciation of a mineral by shifting chemical equilibria if ions of the electrolyte are also constituents of a semi-soluble mineral in contact with the aqueous phase [89]. For example, in the case of CaF_2, the presence of soluble fluoride in the bulk liquid phase leads to a substitution of surface hydroxyls, which are essential for the adsorption of carboxylate species [34] by fluoride ions. Despite these changes in surface composition, it has been demonstrated by electrokinetic measurements that the overall electrostatic structure of fluoride minerals is not much affected by the presence of moderate fluoride concentrations because of the strong hydration of fluoride ions in aqueous environments [99]. A comparison of the effect of two monovalent electrolytes, NaCl(aq) and NaF(aq), on acetate adsorption at the fluorite–water interface was used to elucidate the role of specific interactions between adsorbates and surface sites [29]. NaCl is lacking any common constituents with CaF_2 and is thus unlikely to affect surface speciation of fluoride, but will however be similar to NaF as far as the action of these electrolytes in the diffuse electrostatic layer at the interface is concerned.

By using VSFS, the amount of substrate–adsorbed acetate has been determined at various chloride and fluoride concentrations (figures 8(*a*) and (*b*)). These experiments [29] revealed that the presence of chloride ions, even at concentrations as high as 150 mM, hardly affects acetate adsorption at the CaF_2–water interface, as can be concluded from the only moderately changing carboxylate amplitude of figure 8(*a*). On the contrary, fluoride ions effectively

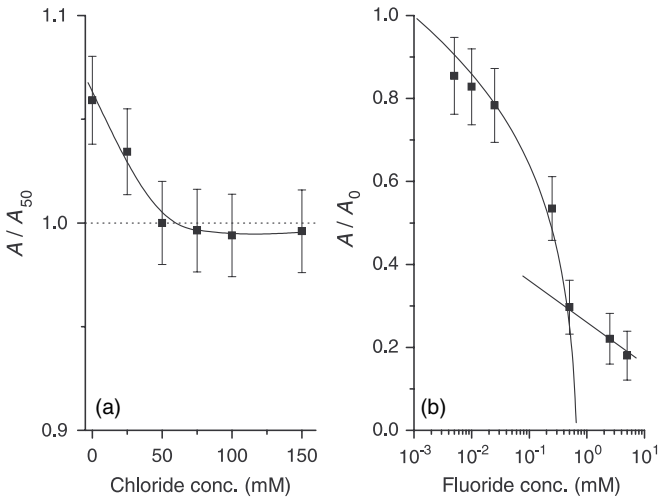

Figure 8. (*a*) Combined VSF amplitude of the carboxylate bands A as a function of bulk chloride concentration (in mM), normalized by the amplitude at 50 mM sodium chloride (aq), A_{50}. (*b*) Normalized amplitude A/A_0 as a function of fluoride concentration (in μM). A_0 corresponds to the sample without added fluoride. Curves show trends only. Reprinted with permission from [29]. Copyright 2007 American Chemical Society.

reduce acetate adsorption already at millimolar concentrations, when substitution of surface hydroxyls by F^- commences (at ~0.3 mM, figure 8(*b*)) [89]. This was attributed to the protonated surface hydroxyls forming more stable associates with carboxylates than with fluoride containing surface species [29, 34].

Common experimental approaches, e.g. electrokinetic measurements [93, 99], probe the overall electrostatic structure of the interface rather than microscopic details at the mineral surface, and only small effects of millimolar fluoride concentrations on the zeta potential of CaF_2 were reported [99]. Using (non-linear) spectroscopic techniques, it can be shown that the adsorbate-substrate interactions very much depend on the specific surface chemistry and microscopic charge distribution, even if these interactions are not associated with covalent bonding or a change of the macroscopic electrostatic behaviour at the interface [29, 34].

9. Dynamic aspects

Only very recently have VSFS studies at the mineral–water interface been extended to dynamic aspects of adsorbate layers [114, 115]. Besides the kinetics of adsorption and desorption of surface active agents, equilibrium exchange dynamics are of particular interest because they allow the dynamics of substrate–adsorbate interactions and effects of interfacial water structure to be investigated. Isotopical labelling of the alkyl chain has proven useful for monitoring monomer exchange of self-assembled dodecanoate monolayers deposited on fluorite [114]. Figure 9 shows results of a typical experiment, where the (constant) adsorption density was continuously monitored by the carboxylate signal at 1453 cm^{-1} (figure 9(*a*)). At first, the equilibrium monolayer is composed of deuterated surfactant only ($t < t_0$, figure 9(*b*)). Then, the bulk liquid is replaced by a solution containing fully hydrogenated

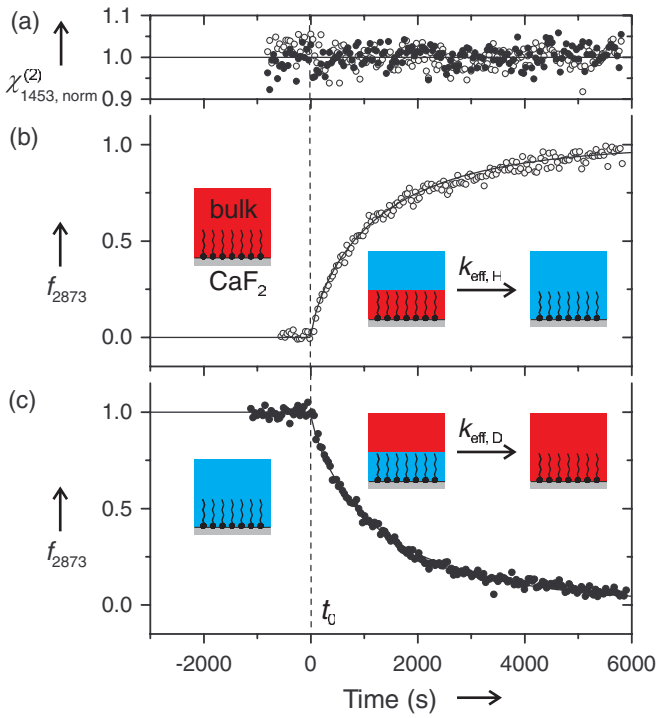

Figure 9. (*a*) Monomer exchange kinetics of sodium dodecanoate at the fluorite–water interface (circles: fully deuterated, bullets: fully hydrogenated monolayer for $t < t_0$). (*a*) Normalized non-linear optical response of the carboxylate headgroup, $\chi^{(2)}_{1453,norm}$. (*b*) Exchange kinetics ($k_{eff,H}$) of a deuterated monolayer and (*c*), of a hydrogenated monolayer ($k_{eff,D}$). f_{2873} is the mole fraction of hydrogenated surfactant in the monolayer. At t_0, the bulk liquid phase was replaced by a surfactant solution of equal concentration (10 μM) but opposite isotope labelling. In the pictorial representations, blue/dark grey areas correspond to hydrogenated, red/light grey areas to deuterated surfactant molecules. Reprinted from [114] with permission of Wiley-VCH, Weinheim. (Colour online.)

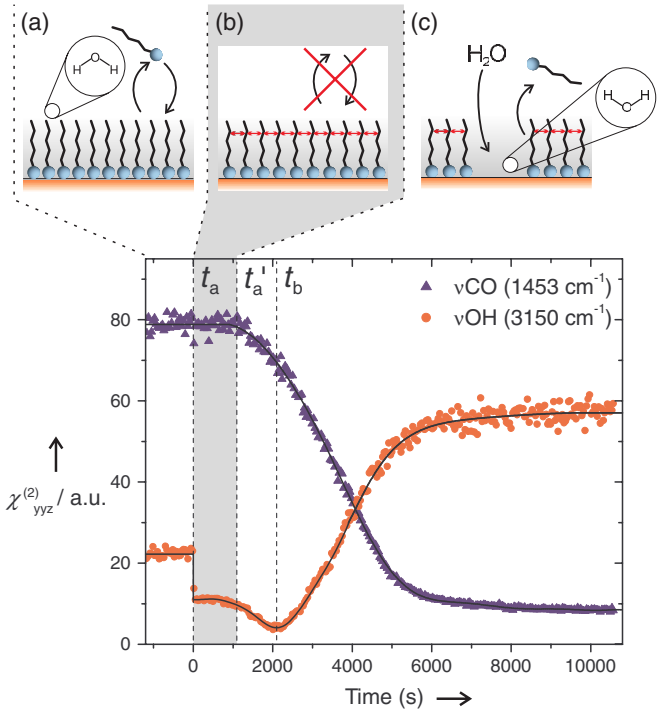

Figure 10. Desorption kinetics of an equilibrated dodecanoate monolayer. At time t_a, the surfactant solution was replaced by neat water. Surface coverage is followed by the νCO response at 1453 cm^{-1} (blue triangles) and remains virtually constant until t_a'. At t_b, the phase of the νOH resonance (red bullets) shifts by π, indicating a flip of the interfacial water molecules due to surface charge reversal. Also given is a schematic view of the monolayer (*a*) in equilibrium with a bulk surfactant solution, (*b*) during the induction period (grey area; arrows indicate a non-equilibrium state of the monolayer) and (*c*) during desorption. The predominant orientation of water molecules above the monolayer and at the CaF_2 surface is also shown. Reprinted from [114] with permission of Wiley-VCH, Weinheim. (Colour online.)

surfactant only. A change in the signal at 2873 cm^{-1} (CH_3 symmetric stretch) is observed, which reflects the kinetics of monomer substitution in the monolayer. Following the same experimental protocol, kinetic data can also be obtained starting from a fully hydrogenated monolayer (figure 9(*c*), and a comparison of monomer exchange rates, together with an idealized model of the exchange mechanism revealed intricate details of the exchange process [114].

Studies on adsorption and desorption processes are still work in progress [115], but a first account is due to appear soon [114]. Figure 10 shows the different stages of desorption of a dodecanoate monolayer deposited on fluorite. In this experiment, the surface density of oriented surfactant molecules was monitored by their response at 1453 cm^{-1} (carboxylate headgroup), while the number of water molecules aligned by the interfacial field was probed by their sum-frequency signal at 3150 cm^{-1}. In equilibrium, both signals are constant, albeit dynamic exchange of monomers occurs at the interface (figure 10(*a*)). At t_a, desorption was initiated by flushing the fluorite surface with neat water instead of bulk surfactant solution. While the surface density of surfactant remains nearly unchanged until t_a', the response arising from interfacial water molecules instantaneously drops to about half of its value under equilibrium conditions. This change cannot be explained simply by the variation of the ionic strength associated with the substitution of the (μmolar) surfactant solution in contact with the equilibrium monolayer by neat water. It was concluded that the structure of the interfacial layer is distinctively different under non-equilibrium conditions (during desorption) compared to its equilibrium state, although this restructuring has little effect on the surface density of the adsorbate. From the nearly constant surface density at $t > t_a$, it can also be inferred that the release of monomers from the monolayer stops if defects in the monolayer generated by this process cannot be readily replenished by adsorption from the liquid phase. The high energetic cost arising from water–alkyl contacts at defects was held responsible for the slowing-down of monomer release. After some time however (t_a', figure 10(*c*)), the slowly growing number of monolayer defects reaches a critical limit. Desorption was then described to proceed much faster, e.g. along the boundaries of such defects, while direct water–fluorite contacts are reestablished. At t_b, the net orientation of water molecules at the interface vanishes. The experiments [114] also revealed that the orientation of water molecules above the monolayer is opposite to that on fluorite.

10. Conclusions and outlook

This topical review summarizes efforts to investigate adsorption at mineral–water interfaces by non-linear optical spectroscopy. The strength and limitations of this inherently surface-specific technique are addressed. Because of its ability to probe vibrational transitions, VSFS has found considerable use especially for the study of molecular adsorbates. Arguably, its sensitivity for water structuring at interfaces is unparalleled by other experimental approaches.

So far, most non-linear spectroscopic work at mineral–water interfaces have focused on fluorite (CaF_2), which has been regarded as a typical representative of ionic solids. From studies of the adsorption characteristics of a homologous series of carboxylates, from formate (C_1) up to stearate (C_{18}), a detailed picture of interfacial structure has been developed. These studies show that electrostatics is an important driving mechanism for the adsorption of small organic ions at this interface, but as soon as adsorbates containing significant hydrophobic moieties are involved, Van-der-Waals and hydrogen-bond mediated interactions become more important. Non-linear optical spectroscopies also make information on conformational order of adsorbate layers and molecular orientation of water molecules at various stages of adsorption directly accessible. Using such data, the mechanism of bilayer formation of SDS was elucidated, and for the more well-ordered carboxylate monolayers, three distinct hydrogen-bonding environments were observed in the interfacial layer.

Our understanding of these interfaces is not complete as long as molecular-scale data are limited to the static case and equilibrium interfaces. Compared with processes in bulk liquids, adsorption and aggregation on solids typically exhibit quite slow kinetics. Such slow processes are responsible for many time-dependent properties of solid–liquid heterogeneous systems and govern—apart from many other phenomena—stability and rheology of suspensions. VSFS appears to be one of the most promising ways to elucidate the structure of the intricate non-equilibrium interfacial structures and thus of the molecular pathways of adsorption and desorption processes.

First accounts of dynamic studies already showed that self-assembled monolayers formed by surfactant adsorption on minerals, which have so far often been considered irreversibly bonded, are constantly exchanging monomers with the bulk solution in equilibrium. Moreover, the energy barriers associated with this exchange process strongly depend upon the hydrogen-bond structure close to the interface, which has been probed by the sum-frequency signal arising from the OH stretch of oriented water molecules. If the equilibrium state is disturbed (e.g. during desorption), the rate of surfactant release is nearly zero until coverage drops below a critical limit.

Apart from non-equilibrium surface states, electrolytes are frequently encountered in aqueous phases found in nature and industry. The importance of ionic solutes for interfacial processes has long been recognized, but much remains to be learned about their specific actions at interfaces, and the contribution from non-linear optical methods might be critical to advance this field. These studies described herein are beginning to provide insight into fundamental issues underlying such processes at the CaF_2/H_2O interface. Many opportunities for expanding such studies to a broader range of mineral surfaces are possible in the future.

Acknowledgments

Financial support for this work was provided by the Department of Energy, Basic Energy Sciences, Grant DEFG02-96ER45557, and is gratefully acknowledged. SS appreciates a scholarship of the German Research Foundation (DFG, Bonn).

References

[1] Roberts W M 1981 *Chem. Br.* **17** 510
[2] Fenter P and Sturchio N C 2004 *Prog. Surf. Sci.* **77** 171
[3] Möbius D and Miller R 2001 *Novel Methods to Study Interfacial Layers* (Amsterdam: Elsevier)
[4] Somasundaran P and Kunjappu J T 1988 *Miner. Metall. Process.* **5** 68
[5] Hall R B and Ellis A B 1986 *Chemistry and Structure at Interfaces* (Deerfield Beach, FL: VCH)
[6] Binks B P 1999 *Modern Characterization Methods of Surfactant Systems* (New York: Dekker)
[7] Brady P V 1996 *Physics and Chemistry of Mineral Surfaces* (Boca Raton, FL: CRC Press)
[8] Chandar P, Somasundaran P and Turro N J 1987 *J. Colloid Interface Sci.* **117** 31
[9] Free M L and Miller J D 1997 *Langmuir* **13** 4377
[10] Neivandt D J, Gee M L, Hair M L and Tripp C P 1998 *J. Phys. Chem.* B **102** 5107
[11] Richmond G L 2002 *Chem. Rev.* **102** 2693
[12] Piletic I R, Moilanen D E, Levinger N E and Fayer M D 2006 *J. Am. Chem. Soc.* **128** 10366
[13] Guyot-Sionnest P, Hunt J H and Shen Y R 1987 *Phys. Rev. Lett.* **59** 1597
[14] Hirose C, Yamamoto H, Akamatso N and Domen K 1993 *J. Phys. Chem.* **97** 10064
[15] Wolfrum K, Löbau J and Laubereau A 1994 *Appl. Phys.* A **59** 605
[16] Zhuang X, Miranda P B, Kim D and Shen Y R 1999 *Phys. Rev.* B **59** 12632
[17] Shen Y R 1984 *The Principles of Nonlinear Optics* (Wiley: New York)
[18] Shen Y R 1989 *Ann. Rev. Phys. Chem.* **40** 327
[19] Bain C D 1995 *J. Chem. Soc. Faraday Trans.* **91** 1281
[20] McGilp J F 1996 *J. Phys. D: Appl. Phys.* **29** 1812
[21] Buck M and Himmelhaus M 2001 *J. Vac. Sci. Technol.* A **19** 2717
[22] Raschke M B and Shen Y R 2004 *Curr. Opin. Solid State Mater. Sci.* **8** 343
[23] Superfine R, Guyot-Sionnest P, Hunt J, Kao C T and Shen Y R 1988 *Surf. Sci.* **200** L445
[24] Bell G R, Bain C D and Ward R N 1996 *J. Chem. Soc. Faraday Trans.* **92** 515
[25] Hirose C, Akamatsu N and Domen K 1992 *Appl. Spectrosc.* **46** 1051
[26] Bain C D, Davies P B, Hui Ong T, Ward R N and Brown M A 1991 *Langmuir* **7** 1563
[27] Goates S R, Schofield D A and Bain C D 1999 *Langmuir* **15** 1400
[28] Moore F G, Becraft K A and Richmond G L 2002 *Appl. Spectrosc.* **56** 1575
[29] Schrödle S, Moore F G and Richmond G L 2007 *J. Phys. Chem.* C **111** 10088

[30] Williamsa C T and Beattie D A 2002 *Surf. Sci.* **500** 545
[31] Woodruff D P and Delchar T A 1994 *Modern Techniques of Surface Science* (Cambridge: Cambridge University Press)
[32] Yates, Jr J T 1998 *Experimental Innovations in Surface Science: a Guide to Practical Laboratory Methods and Instruments* (Berlin: Springer)
[33] Freund H J and Umbach E 1993 *Adsorption on Ordered Surfaces of Ionic Solids and Thin Films* (Berlin: Springer)
[34] Holmgren A, Wu L and Forsling W 1994 *Spectrochim. Acta* A **50A** 1857
[35] Drelich J, Atia A A, Yalamanchili M R and Miller J D 1996 *J. Colloid Interface Sci.* **178** 720
[36] Drelich J, Jang W H and Miller J D 1997 *Langmuir* **13** 1345
[37] Mielczarski E, Mielczarski J A and Cases J M 1998 *Langmuir* **14** 1739
[38] Parekh B K and Miller J D 1999 *Advances in Flotation Technology* (Littleton, CO: Society for Mining, Metallurgy, and Exploration)
[39] Mielczarski E, de Donato P, Mielczarski J A, Cases J M, Barres O and Bouquet E 2000 *J. Colloid Interface Sci.* **226** 269
[40] Mielczarski E and Mielczarski J A 2002 *C. R. Geoscience* **334** 703
[41] Atkin R, Craig V S J, Wanless E J and Biggs S 2003 *Adv. Colloid Interface Sci.* **103** 219
[42] Johnson S B, Yoon T H, Kocar B D and Brown G E Jr 2004 *Langmuir* **20** 4996
[43] Johnson S B, Yoon T H, Slowey A J and Brown G E Jr 2004 *Langmuir* **20** 11480
[44] Yoon T H, Johnson S B, Musgrave C B and Brown G E Jr 2004 *Geochim. Cosmochim. Acta* **68** 4505
[45] Johnson S B, Yoon T H and Brown G E Jr 2005 *Langmuir* **21** 2811
[46] Lyklema J 2006 *Colloids Surf.* A **291** 3
[47] Zolk M, Eisert F, Pipper J, Herrwerth S, Eck W, Buch M and Grunze M 2000 *Langmuir* **16** 5849
[48] Ostroverkhov V, Waychunas G A and Shen Y R 2004 *Chem. Phys. Lett.* **386** 144
[49] Becraft K A, Moore F G and Richmond G L 2003 *J. Phys. Chem.* B **107** 3675
[50] Becraft K A, Moore F G and Richmond G L 2004 *Phys. Chem. Chem. Phys.* **6** 1880
[51] Becraft K A and Richmond G L 2005 *J. Phys. Chem.* B **109** 5108
[52] Kataoka S, Gurau M C, Albertorio F, Holden M A, Lim S M, Yang R D and Cremer P S 2004 *Langmuir* **20** 1662
[53] Yaganeh M S, Dougal S M and Pink H S 1999 *Phys. Rev. Lett.* **83** 1179–82
[54] Becraft K A and Richmond G L 2001 *Langmuir* **17** 7721
[55] Kuroda Y, Kittaka S, Takahara S, Yamaguchi T and Bellissent-Funel M C 1999 *J. Phys. Chem.* B **103** 11064
[56] Takahara S, Kittaka S, Mori T, Kuroda Y, Yamaguchi T and Shibata K 2002 *J. Phys. Chem.* B **106** 5689
[57] Mamontov E 2004 *J. Chem. Phys.* **121** 9087
[58] Mamontov E 2005 *J. Chem. Phys.* **123** 171101
[59] Mamontov E 2005 *J. Chem. Phys.* **123** 024706
[60] Mamontov E, Vlcek L, Wesolowski D J, Cummings P T, Wang W, Anovitz L M, Rosenqvist J, Brown C M and Garcia Sakai V 2007 *J. Phys. Chem.* C **111** 4328
[61] Yegameh M S, Dougal S M and Pink H S 1999 *Phys. Rev.Lett.* **83** 1179
[62] Brown G E Jr *et al* 1999 *Chem. Rev.* **99** 77
[63] Du Q, Superfine R, Freysz E and Shen Y R 1993 *Phys. Rev. Lett.* **70** 2313
[64] Du Q, Freysz E and Shen Y R 1994 *Science* **264** 826
[65] Du Q, Freysz E and Shen Y R 1994 *Phys. Rev. Lett.* **72** 238
[66] Gragson D E and Richmond G L 1998 *J. Am. Chem. Soc.* **120** 366
[67] Hopkins A J, McFaerin C L and Richmond G L 2005 *Curr. Opin. Solid State Mater. Sci.* **9** 19
[68] Raymond E A, Tarbuck T L and Richmond G L 2002 *J. Phys. Chem.* B **106** 2817
[69] Ye S, Nihonyanagi S and Uosaki K 2001 *Phys. Chem. Chem. Phys.* **3** 3463
[70] Gurau M C, Kim G, Lim S M, Albertorio F, Fleisher H C and Cremer P S 2003 *ChemPhysChem* **4** 1231
[71] Grosberg A Y, Nguyen T T and Shklovskii B I 2002 *Rev. Mod. Phys.* **74** 329
[72] Faraudo J and Travesset A 2007 *J. Phys. Chem.* C **111** 987
[73] Luo G, Malkova S, Yoon J, Schultz D G, Lin B, Meron M, Benjamin I, Vanýsek P and Schlossman M L 2006 *Science* **311** 216
[74] Debye P and Hückel E 1923 *Phys. Z.* **24** 185
[75] Safran S A 1994 *Statistical Thermodynamics of Surfaces, Interfaces, and Membranes* (New York: Perseus)
[76] Israelachvili J and Wennerström H 1996 *Nature* **379** 219
[77] Al-Abadleh H A, Voges A B, Bertin P A, Nguyen S T and Geiger F M 2004 *J. Am. Chem. Soc.* **126** 11126
[78] Al-Abadleh H A, Mifflin A L, Bertin P A, Nguyen S T and Geiger F M 2005 *J. Phys. Chem.* B **109** 9691
[79] Al-Abadleh H A, Mifflin A L, Musorrafiti M J and Geiger F M 2005 *J. Phys. Chem.* B **109** 16852
[80] Rubingh D N and Holland P M 1990 *Cationic Surfactants: Physical Chemistry* (New York: Dekker)
[81] Sharma R 1995 *Surfactant Adsorption and Surface Solubilization* (Washington, DC: American Chemical Society)
[82] Young C A and Miller J D 2000 *Int. J. Miner. Process.* **58** 331
[83] Schrödle S, Moore F G and Richmond G L 2007 *J. Phys. Chem.* C **111** 8050
[84] Graustein W C, K Cromack J and Sollins P 1977 *Science* **198** 1252
[85] Strobel B W 2001 *Geoderma* **99** 169
[86] Davis J A and Hayes K F 1986 *Geochemical Processes at Mineral Surfaces* (Washington, DC: American Chemical Society)
[87] Schnitzer M 2000 *Adv. Agron.* **68** 1
[88] Wu L, Forsling W and Schindler P W 1991 *J. Colloid Interface Sci.* **147** 178
[89] Wu L and Forsling W 1995 *J. Colloid Interface Sci.* **174** 178
[90] Gonzálz-Martín M L, Jańczuk B and Bruque J M 1995 *J. Therm. Anal.* **44** 1087
[91] de Leeuw N H and Cooper T G 2003 *J. Mater. Chem.* **13** 93
[92] Wu L, Forsling W and Holmgren A 2000 *J. Colloid Interface Sci.* **224** 211
[93] Miller J D, Fa K, Calara J V and Paruchuri V K 2004 *Colloids Surf.* A **238** 91
[94] Assemi S, Nalaskowski J, Miller J D and Johnson W P 2006 *Langmuir* **22** 1403
[95] Gragson D E and Richmond G L 1998 *J. Phys. Chem.* B **102** 3847
[96] Gaudin A M and Fuerstenau D W 1955 *Trans. AIME* **202** 958
[97] Mielczarski J A, Mielczarski E and Cases J M 1999 *Langmuir* **15** 500
[98] Li H and Tripp C P 2002 *Langmuir* **18** 9441–6
[99] Hu Y, Lu Y, Veeramasuneni S and Miller J D 1997 *J. Colloid Interface Sci.* **190** 224
[100] Miranda P B, Pflumio V, Saijo H and Shen Y R 1998 *Thin Solid Films* **327–329** 161
[101] Miranda P B, Pflumio V, Saijo H and Shen Y R 1998 *J. Am. Chem. Soc.* **120** 12092
[102] Johnson C M and Tyrode E 2005 *Phys. Chem. Chem. Phys.* **7** 2635
[103] Hore D K, Beaman D K and Richmond G L 2005 *J. Am. Chem. Soc.* **127** 9356

[104] Hore D K, Beaman D K and Richmond G L 2005 *J. Phys. Chem.* B **109** 16846
[105] Ward R N, Duffy D C, Davies P B and Bain C D 1994 *J. Phys. Chem.* B **98** 8536
[106] Windsor R, Neivandt D J and Davies P B 2001 *Langmuir* **17** 7306
[107] Liu Y, Wolf L K and Messmer M C 2001 *Langmuir* **17** 4329
[108] Watry M R and Richmond G L 2002 *Langmuir* **18** 8881
[109] Hiemstra T and van Riemsdijk W H 1996 *J. Colloid Interface Sci.* **179** 488
[110] Criscenti L J and Sverjensky D A 2002 *J. Colloid Interface Sci.* **253** 329
[111] Sverjensky D A 2001 *Geochim. Cosmochim. Acta* **65** 3643
[112] Zhang Z *et al* 2004 *Langmuir* **20** 4954
[113] Zhang Z, Fenter P, Cheng L, Sturchio N C, Bedzyk M J, Machesky M L and Wesolowski D J 2004 *Surface Sci.* **554** L95
[114] Schrödle S and Richmond G L 2007 *ChemPhysChem* **8** 2315
[115] Schrödle S and Richmond G L 2007 submitted